Chirality

An Isosteric Triaza Analogue of a Polycyclic Aromatic Hydrocarbon Monkey Saddle

Tobias Kirschbaum, Frank Rominger, and Michael Mastalerz*[a]

Dedicated to Professor Günter Helmchen on the occasion of his 80th birthday.

Abstract: Since a few years, the interest in negatively-curved fused polycyclic aromatic hydrocarbons (PAHs) has significantly increased. Recently, the first chiral negatively-curved PAH with the topology of a monkey saddle was introduced. Herein the synthesis of its triaza congener is reported. The influence of this CH↔N exchange on photophysical and electrochemical properties is studied as well as the isomerization process of the enantiomers. The aza analogue has a significantly higher inversion barrier, which makes it easier to handle at room temperature. All experimental results are underpinned by theoretical DFT calculations.

The interest in curved polycyclic aromatic hydrocarbons (PAHs) has increased significantly in the last years.[1] One can distinguish between positively- and negatively-curved PAHs. The positively-curved PAHs, such as fullerenes, corannulene or other buckybowls, usually contain one or more pentagonal rings besides hexagonal ones.[2,3] In contrast, those PAHs with a negative curvature are generated by the incorporation of heptagonal or octagonal rings.[1c,4–6] The simplest negatively-curved PAH is [7]circulene, which was first time synthesized in 1988 by Yamamoto et al.[7] The next higher homologue with negative curvature, the [8]circulene was not yet synthesized, but in 2013 a larger derivative, the tetrabenzo[8]circulene was presented.[5b–d] Since then the field experienced a real renaissance.[1] Contorted PAHs are more soluble than their comparable planar congeners, because packing of those molecules by tight π-stacking is largely reduced due to the intrinsic curvature. Furthermore, photophysical and electrochemical properties of contorted PAHs are different than those of planar compounds, and significantly depending on the degree of contortion.[8,9] Last but not least, such planar PAHs are molecularly precise cutout structures of graphene; curved PAHs are cutout structures of three-dimensional conjugated PAHs, such as Mackay crystals,[10] with distinguished new materials properties.[11] Similar to smaller planar PAHs, they can be reacted in a controlled manner to produce larger ones or graphene nanoribbons (GNRs);[12] contorted PAHs in principle can be reacted to form curved fully conjugated PAH cages or even to well-ordered crystals. No doubt, these goals are synthetically quite challenging, but offer the exploration of new types of conjugated molecules and materials with yet unprecedented properties.[13]

In contrast to planar PAHs, contorted PAHs with *N*-heterocyclic units are much rarer.[14–16] There have been a few examples of positively-curved buckybowls and related structures, containing *N*-heterocyclic subunits.[15,17] Most of these structures include pyrrole rings and therefore it is not surprising that for the majority of those structures no isosterical pure CH-analogues are known to compare properties, such it is for example, the case for planar acenes and heteroacenes.[18] A rare exception is the couple sumanene-triazasumanene,[17q,19] whereas isosteric azacorannulenes seem not to be stable and decompose to other products, accompanied by the loss of curvature.[17b,20] To the best of our knowledge, for negatively-curved PAHs, no such isosteric couple was described to date.

Recently we introduced the first monkey saddle shaped PAH **1** (we will abbreviate this compound as CH-MS **1**), which is conformationally[1c,4a,j–l] stable at ambient conditions.[21] This monkey saddle PAH consists besides seven hexagons, of three pentagonal and three octagonal rings. Among all possible isosteric C_3-symmetric triaza monkey saddle PAHs (for detailed analysis of frontier molecular orbital energies, see Supporting Information), the largest difference in stabilization of HOMO and LUMO energies is found for the aza monkey saddle **2** (we will abbreviate this compound as aza-MS **2**), where the nitrogen is part of the eight membered ring (Figure 1). In contrast to **1**, the LUMO for **2** is lowered about −0.48 eV from −1.90 to −2.38 eV and the HOMO from −5.23 to −5.64 eV (Table 1). Note that for **1**, two energetically degenerated HOMOs and one HOMO-1 are calculated, whereas for aza-MS **2**, this situation switches: Here we have only one HOMO and two degenerated HOMO-1 levels (−5.71 eV). By calculations of the anisotropy of the induced current density (AICD-plot) and nucleus-independent chemical shift (NICS) values it is suggested that ring currents of several rings change only marginal and thus

[a] T. Kirschbaum, Dr. F. Rominger, Prof. Dr. M. Mastalerz
Organisch-Chemisches Institut
Ruprecht-Karls-Universität Heidelberg
Im Neuenheimer Feld 270, 69120 Heidelberg (Germany)
E-mail: michael.mastalerz@oci.uni-heidelberg.de

Supporting information and the ORCID identification number(s) for the author(s) of this article can be found under:
https://doi.org/10.1002/chem.202002826.

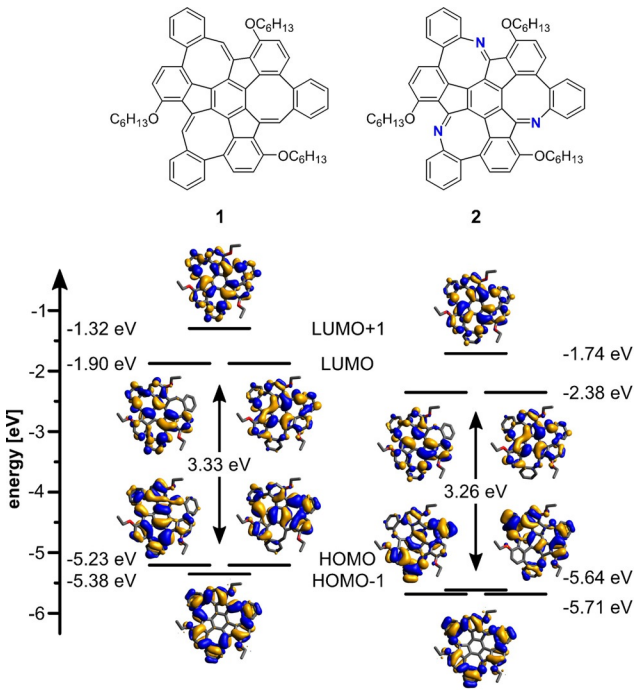

Figure 1. Comparison of DFT calculated molecular orbitals (B3LYP/6–311G(d,p)) of monkey saddle PAH **1** and aza-monkey saddle PAH **2**.

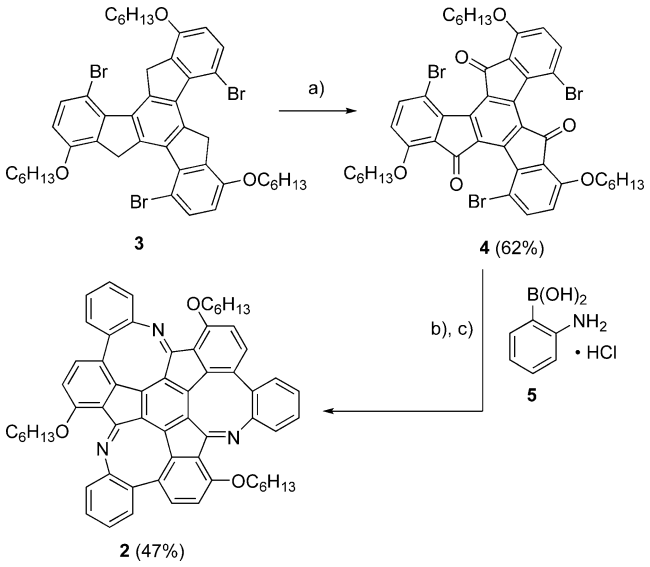

Scheme 1. Synthesis of aza monkey saddle PAH **2**. a) O_2, K_2CO_3, DMF, 40 °C, 96 h; b) 5 mol% Pd_2dba_3, 20 mol% $H(tBu)_3PBF_4$, 21 equiv K_2CO_3, THF/H_2O (1:1 v/v), 80 °C, 48 h; c) 10 vol% AcOH, $CHCl_3$, 80 °C, 18 h.

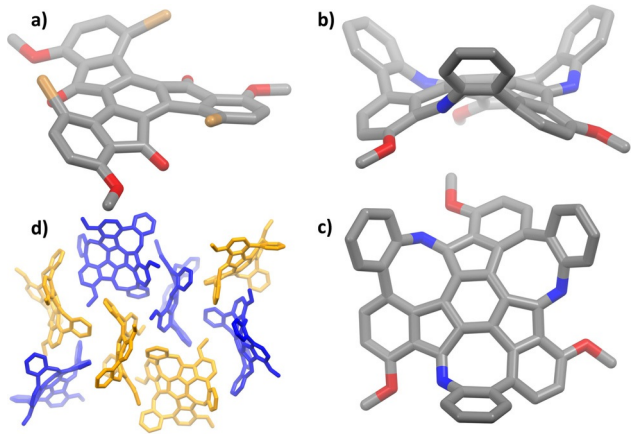

Figure 2. Single-crystal X-ray structures of a) bromotruxenone **4** and b–d) aza-MS **2**. In a) only the (*M,M,M*)- enantiomer and in b) and c) only the (S_a,S_a,S_a)-enantiomer is depicted. d) Packing of aza-MS **2** in the unit cell. (S_a,S_a,S_a) enantiomers are displayed in yellow and (R_a,R_a,R_a) in blue. In all structures, solvent molecules and hydrogen atoms are omitted as well as the hexyloxy chains reduced to the first carbon connected to oxygen for clarity.

the overall stability of aza-MS **2** is comparable to that of the hydrocarbon congener **1** (see Table S2 and Figure S36 in the Supporting Information).

Aza-MS **2** was synthesized in two steps from bromotruxene **3** (Scheme 1),[21] which was oxidized with oxygen in the presence of K_2CO_3 in DMF to the corresponding truxenone **4** (62% yield).[22] The second and final step was a cross-coupling with the HCl salt of aniline boronic acid **5**, followed by treatment with acetic acid (10 vol%) in $CHCl_3$ at 80 °C to give the title compound **2** after column chromatography as a bright orange powder in 47% isolated yield (over both steps). Aza-MS **2** was fully characterized (for details, see the Supporting Information). Besides NMR spectra, the MALDI TOF MS gave the information of a successful formation of **2** by a fitting peak at m/z = 904.4482 $[M+H]^+$. In the IR spectrum no stretching band for a C=O is found; instead a clear band at 1645 cm^{-1} was detected, which is in the typical range of C=N imine vibrations.

From both, bromotruxenone **4** and the aza-MS **2**, single crystals of high quality were obtained (Figure 2). Bromotruxenone **4** crystallized in the orthorhombic space group *Pbca*. Due to steric repulsion of the bromo and the carbonyl oxo atoms (average d_{Br-O} = 3.03 Å) the molecule is triply helically twisted out of plane by about 47°. Both (*M,M,M*) and (*P,P,P*) enantiomers are found. The aza-MS **2** crystallized as racemic crystal with both enantiomers (R_a,R_a,R_a) and (S_a,S_a,S_a) found in the asymmetric unit of the monoclinic space group $P2_1/c$. Most in-

Table 1. Comparison of key-data of monkey saddle PAH **1** and aza monkey saddle PAH **2**.

Cpnd	$E_{LUMO,DFT}$ [eV]	$E_{HOMO,DFT}$[a] [eV]	$E_{IP,CV}$[b] [eV]	$E_{EA,CV}$[b] [eV]	$E_{gap,CV}$ [eV]	λ_{max} [nm]	λ_{onset} [nm]	$E_{gap,opt}$ [eV]	$E_{Arrac,\ DFT}$ [kJ mol^{-1}]	$E_{Arrac,\ exp}$ [kJ mol^{-1}]	$t_{1/2}$ @70 °C
CH-MS **1**	−1.90	−5.23	−5.45	−3.0	2.5	280	490	2.5	102	104 ± 4 6	6.9 ± 0.4 min
aza-MS **2**	−2.38	−5.65	−5.65	−3.3	2.4	273	520	2.4	112	113 ± 6	7.7 ± 0.1 h

[a] B3LYP/6–311G(d,p). [b] 1 mM in DCM; scan speed: 100 mV s^{-1}; Fc/Fc^+ was used as internal reference.[24] $E_{CV=}-(E_{onset}+5.1\ eV)$.

teresting is the comparison of the degree of contortion with that of the CH-MS **1**.[21] The angle between the unsubstituted rings and the central one is between 41.9° and 48.1°. Between the hexyloxy substituted rings and the central ring the angles are between 29.0° and 36.4°. These values are very similar to the ones observed for the hydrocarbon monkey saddle **1** (40.6 to 52.9° and 28.1 to 33.6°). This extraordinary structural similarity predestines this pair of compounds to study the isosterical exchange of one CH unit by nitrogen on molecular properties for negatively contorted PAHs.

The UV/Vis spectrum in CH_2Cl_2 of the aza-MS **2** is a bit less pronounced than the one of CH-MS **1** (Figure 3). It shows three maxima at $\lambda_1 = 273$ nm ($\varepsilon_1 = 63\,516\ M^{-1}cm^{-1}$), $\lambda_2 = 316$ nm ($\varepsilon_2 = 26\,900\ M^{-1}cm^{-1}$), and $\lambda_3 = 414$ nm ($\varepsilon_3 = 13\,631\ M^{-1}cm^{-1}$). The onset is in comparison to **1** slightly bathochromically shifted to $\lambda_{onset} = 520$ nm, which corresponds to an optical band gap of $E_{gap,opt} = 2.4$ eV, which is negligible smaller than for **1** ($E_{gap,opt} = 2.5$ eV; $\lambda_{onset} = 490$ nm) and follows the trend of the DFT calculation (see above). In a mixture of DCM/TFA, the solution of MS **2** became pale red and showed a broadening of the longest wavelength, peak shifting bathochromically to an onset at $\lambda_{onset} = 710$ nm, which can be explained by protonation of the three sp^2-hybridized nitrogens of the azocine rings. The protonation is reversible. By addition of an excess of triethylamine the spectrum matches the original one (see Supporting Information). As expected, the addition of TFA has no effect to the adsorption spectrum of CH-MS **1**.

Both monkey saddle PAHs were compared by cyclovoltammetry under the same conditions (for details see the Supporting Information). The CH-MS **1** shows an irreversible oxidation at +0.65 V, whereas the aza-MS **2** is oxidized at higher potentials (+0.85 V). This corresponds to ionization potentials of −5.45 eV (**1**) and −5.65 eV (**2**) and matches the trend of the DFT calculated stabilization of the HOMO. The first reduction potential of CH-MS **1** is found at −1.8 V (electron affinity = −3.0 eV) and that of the aza-MS **2** at −1.5 V (−3.3 eV). The electrochemical band gaps of $E_{gap,CV} = 2.5$ eV (**1**) and $E_{gap,CV} = 2.4$ eV (**2**) are the same as the optical ones.

To our delight the racemic aza-MS **2** could be separated by chiral column chromatography using a Chiralpak IE™ column (based on amylose *tris* (3,5-dichlorophenylcarbamate)) and *n*-heptane/*i*PrOH (70:30) as eluent (Figure 4). Circular dichroism UV/Vis spectra of both separated enantiomers are mirror-imaged (Figure 5) showing a Cotton effect that is a bit less pronounced than was reported for **1**.[21] The *g*-values of 3.41×10^{-3} (290 nm), -2.70×10^{-3} (343 nm) and -2.52×10^{-3} (360 nm) for **2** are in the same order of magnitude than the ones found for the pure hydrocarbon CH-MS **1**. By TD-DFT (BHandHLYP/6–311-G(d,p)) is assumed that the red graph of the CD-spectrum is of the enantiomer (S_a,S_a,S_a)-**2** and the black one of the opposite enantiomer (R_a,R_a,R_a)-**2**.[23]

With enantiopure aza-MS **2** in hand the inversion barrier was calculated by kinetic measurements of CD spectra at various temperatures (for details, see the Supporting Information). With $E_A = 113 \pm 6$ kJ mol^{-1} the barrier is higher than previously found for the CH-MS **1** ($E_A = 104 \pm 4$ kJ mol^{-1}). The difference of

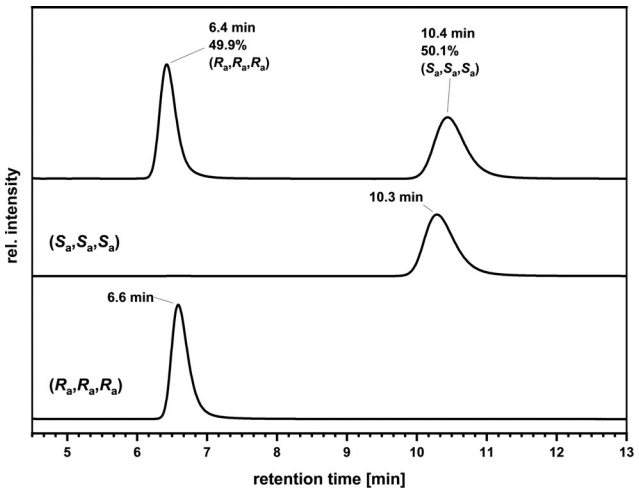

Figure 4. Analytical chiral HPLC traces (IE™ column, *n*-heptane/*i*PrOH 70:30 v/v,1 mL min^{-1}of racemic **2** (top) and separated enantiomers (middle and bottom). The assignment is based on TD-DFT calculations of the corresponding CD spectra (see Figure 5).

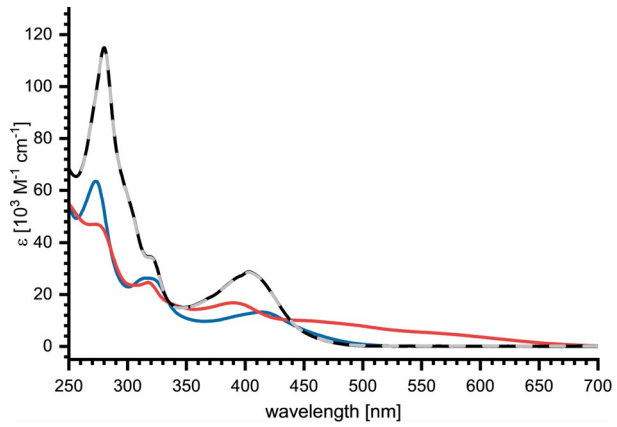

Figure 3. Comparison of UV/Vis of CH-MS **1** (black) and aza-MS **2** (blue) in CH_2Cl_2, before and after addition of TFA (**1** grey; red **2**).

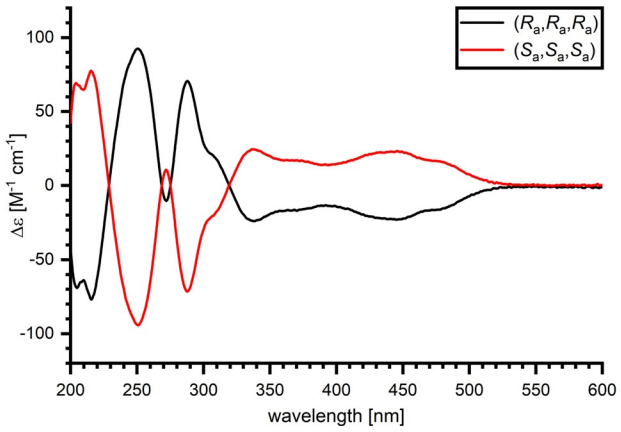

Figure 5. CD spectra of the enantiopure aza-MS **2** (*n*-heptane, (R_a,R_a,R_a): 25 μM, (S_a,S_a,S_a): 21 μM). Assignment of absolute stereochemistry according to TD-DFT calculations (Supporting Information).

+9 kJ mol^{-1} has a significant effect on the half-life times $t_{1/2}$ for the interconversion, shifting from 6.9±0.4 minutes to 7.7±0.1 hours at 70 °C.

The event of racemization of the aza-MS **2** was also investigated by DFT calculations (Figure 6) and compared to that of the CH-MS **1.** As for **1**, it also is most likely a step-wise mechanism via several twisted transition states rather than via a planar one (not depicted). Starting from enantiopure (S_a,S_a,S_a)-**2** the first transition state to intermediate (S_a,S_a,R_a)-**2** is with 103 kJ mol^{-1} nearly the same as calculated for CH-MS **1**. In comparison to (S_a,S_a,R_a)-**1** the intermediate (S_a,S_a,R_a)-**2** is destabilized by 15 kJ mol^{-1}. The second transition state from (S_a,S_a,R_a)-**2** to (R_a,R_a,S_a)-**2** is with 112 kJ mol^{-1} the highest maximum on the reaction coordinate and fits very well to the one calculated by time- and temperature dependent CD spectroscopy (113±6 kJ mol^{-1}), once more underpinning the stepwise mechanism. The higher inversion barrier is best explained by the repulsion of the N and O electron lone pairs of aza-MS **2** being greater than between the more delocalized σ-electrons of the isosteric CH-bond in MS **1**.

In conclusion, a chiral negatively curved nitrogen containing PAH with the shape of a monkey saddle was synthesized in just two steps from bromotruxene **3**. The isosteric substitution of the CH unit of the inherent three cyclooctatetraene rings of CH-MS **1** by nitrogen in aza-MS **2** had the effect of energetically stabilization of the frontier molecular orbitals by about −0.4 eV; a common trend reported for isosteric pairs of PAHs/aza-PAHs.[18a] The stabilization was reflected by higher oxidation and reduction potentials, measured by CV. What clearly distinguishes this negatively curved pair of PAH/ aza-PAH from planar ones is the intrinsic chirality and thus allowed us to study the effect of isosteric exchange of CH-units by nitrogen on the inversion barrier for racemization. The experimentally determined barrier for the aza-MS **2** was with E_A = 113 kJ mol^{-1}, about 10 kJ mol^{-1} higher than previously reported for CH-MS **1**.[21] This prolongs the half-time stability for example, at 70 °C from a few minutes to several hours. This is very important for the further use of derivatives of aza-MS **2** as enantiopure chiral reactant towards the synthesis of Mackay-type cage structures[13]—which is ongoing in our laboratories.

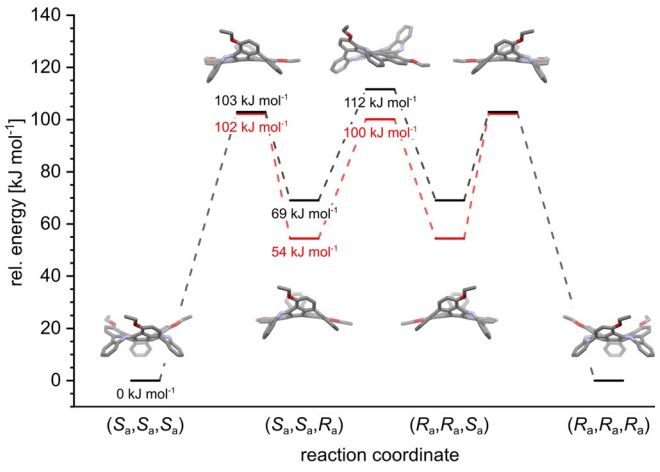

Figure 6. Comparison of reaction paths and calculated barriers (DFT, B3LYP/6–311G(d,p)) for the stereochemical bowl-to-bowl inversion. black: aza-MS **2**; red: CH-MS **1**.

Experimental

Full details of synthesis and characterization of the compounds can be found in the Supporting Information.

Deposition Numbers 1994481 (for **4**) and 1994480 (for **2**) contain the supplementary crystallographic data for this paper. These data are provided free of charge by the joint Cambridge Crystallographic Data Centre and Fachinformationszentrum Karlsruhe Access Structures service www.ccdc.cam.ac.uk/structures.

Acknowledgements

The authors are grateful for funding this project (TP-A04) by Deutsche Forschungsgemeinschaft (DFG) within the collaborative research center SFB 1249 on "*N*-heteropolycycles as functional materials". Support by the state of Baden-Württemberg through bwHPC and the DFG through grant no INST 40/467-1 FUGG (JUSTUS cluster) is acknowledged. Open access funding enabled and organized by Projekt DEAL.

Conflict of interest

The authors declare no conflict of interest.

Keywords: azocine · chirality · monkey saddle · negative curvature · *N*-heteroarenes · polycyclic aromatic hydrocarbons

[1] a) S. H. Pun, Q. Miao, *Acc. Chem. Res.* **2018**, *51*, 1630–1642; b) M. A. Majewski, M. Stępień, *Angew. Chem. Int. Ed.* **2019**, *58*, 86–116; *Angew. Chem.* **2019**, *131*, 90–122; c) I. R. Márquez, S. Castro-Fernández, A. Millán, A. G. Campaña, *Chem. Commun.* **2018**, *54*, 6705–6718; d) Y. Segawa, H. Ito, K. Itami, *Nat. Rev. Mater.* **2016**, *1*, 15002; e) M. Rickhaus, M. Mayor, M. Juríček, *Chem. Soc. Rev.* **2017**, *46*, 1643–1660.

[2] a) V. M. Tsefrikas, L. T. Scott, *Chem. Rev.* **2006**, *106*, 4868–4884; b) Y.-T. Wu, J. S. Siegel, *Chem. Rev.* **2006**, *106*, 4843–4867.

[3] Bharat, R. Bhola, T. Bally, A. Valente, M. K. Cyrański, Ł. Dobrzycki, S. M. Spain, P. Rempała, M. R. Chin, B. T. King, *Angew. Chem. Int. Ed.* **2010**, *49*, 399–402; *Angew. Chem.* **2010**, *122*, 409–412.

[4] a) S. H. Pun, Y. Wang, M. Chu, C. K. Chan, Y. Li, Z. Liu, Q. Miao, *J. Am. Chem. Soc.* **2019**, *141*, 9680–9686; b) S. H. Pun, C. K. Chan, J. Luo, Z. Liu, Q. Miao, *Angew. Chem. Int. Ed.* **2018**, *57*, 1581–1586; *Angew. Chem.* **2018**, *130*, 1597–1602; c) S. Nobusue, K. Fujita, Y. Tobe, *Org. Lett.* **2017**, *19*, 3227–3230; d) X. Gu, H. Li, B. Shan, Z. Liu, Q. Miao, *Org. Lett.* **2017**, *19*, 2246–2249; e) K. Y. Cheung, X. Xu, Q. Miao, *J. Am. Chem. Soc.* **2015**, *137*, 3910–3914; f) K. Kawasumi, Q. Zhang, Y. Segawa, L. T. Scott, K. Itami, *Nat. Chem.* **2013**, *5*, 739; g) C. M. Cruz, S. Castro-Fernández, E. Maçôas, J. M. Cuerva, A. G. Campaña, *Angew. Chem. Int. Ed.* **2018**, *57*, 14782–14786; *Angew. Chem.* **2018**, *130*, 14998–15002; h) C. M. Cruz, I. R. Márquez, S. Castro-Fernández, J. M. Cuerva, E. Maçôas, A. G. Campaña, *Angew. Chem. Int. Ed.* **2019**, *58*, 8068–8072; *Angew. Chem.* **2019**, *131*, 8152–8156; i) C. M. Cruz, S. Castro-Fernández, E. Maçôas, A. Millán, A. G. Campaña, *Synlett* **2019**, *30*, 997–1002; j) H. Chen, Q. Miao, *ChemPlusChem* **2019**, *84*, 627–629; k) K. Y. Cheung, S. Yang, Q. Miao, *Org. Chem. Front.* **2017**, *4*, 699–703; l) K. Y. Cheung, C. K. Chan, Z. Liu, Q. Miao, *Angew. Chem. Int. Ed.* **2017**, *56*, 9003–9007; *Angew. Chem.* **2017**, *129*, 9131–9135; m) Y. Yang, L. Yuan, B. Shan, Z. Liu, Q. Miao, *Chem. Eur. J.* **2016**, *22*, 18620–18627; n) N. Fukui, T. Kim, D. Kim, A. Osuka, *J. Am.*

Chem. Soc. **2017**, *139*, 9075 – 9088; o) N. Fukui, A. Osuka, *Angew. Chem. Int. Ed.* **2018**, *57*, 6304 – 6308; *Angew. Chem.* **2018**, *130*, 6412 – 6416.
[5] a) J.-X. Chen, J.-W. Han, H. N. C. Wong, *Org. Lett.* **2015**, *17*, 4296 – 4299; b) R. W. Miller, A. K. Duncan, S. T. Schneebeli, D. L. Gray, A. C. Whalley, *Chem. Eur. J.* **2014**, *20*, 3705 – 3711; c) Y. Sakamoto, T. Suzuki, *J. Am. Chem. Soc.* **2013**, *135*, 14074 – 14077; d) C.-N. Feng, M.-Y. Kuo, Y.-T. Wu, *Angew. Chem. Int. Ed.* **2013**, *52*, 7791 – 7794; *Angew. Chem.* **2013**, *125*, 7945 – 7948; e) M. Carnes, D. Buccella, T. Siegrist, M. L. Steigerwald, C. Nuckolls, *J. Am. Chem. Soc.* **2008**, *130*, 14078 – 14079.
[6] M. A. Majewski, Y. Hong, T. Lis, J. Gregoliński, P. J. Chmielewski, J. Cybińska, D. Kim, M. Stępień, *Angew. Chem. Int. Ed.* **2016**, *55*, 14072 – 14076; *Angew. Chem.* **2016**, *128*, 14278 – 14282.
[7] K. Yamamoto, T. Harada, Y. Okamoto, H. Chikamatsu, M. Nakazaki, Y. Kai, T. Nakao, M. Tanaka, S. Harada, N. Kasai, *J. Am. Chem. Soc.* **1988**, *110*, 3578 – 3584.
[8] a) X. Yang, F. Rominger, M. Mastalerz, *Angew. Chem. Int. Ed.* **2019**, *58*, 17577 – 17582; *Angew. Chem.* **2019**, *131*, 17741 – 17746; b) A. Bedi, O. Gidron, *Acc. Chem. Res.* **2019**, *52*, 2482 – 2490.
[9] K. Baumgärtner, A. L. Meza Chincha, A. Dreuw, F. Rominger, M. Mastalerz, *Angew. Chem. Int. Ed.* **2016**, *55*, 15594 – 15598; *Angew. Chem.* **2016**, *128*, 15823 – 15827.
[10] A. L. Mackay, H. Terrones, *Nature* **1991**, *352*, 762 – 762.
[11] a) R. Phillips, D. A. Drabold, T. Lenosky, G. B. Adams, O. F. Sankey, *Phys. Rev. B* **1992**, *46*, 1941 – 1943; b) H. Terrones, A. L. Mackay, *Chem. Phys. Lett.* **1993**, *207*, 45 – 50; c) H. Aoki, M. Koshino, D. Takeda, H. Morise, K. Kuroki, *Phys. Rev. B* **2001**, *65*, 035102.
[12] A. Narita, X.-Y. Wang, X. Feng, K. Müllen, *Chem. Soc. Rev.* **2015**, *44*, 6616 – 6643.
[13] M. Tagami, Y. Liang, H. Naito, Y. Kawazoe, M. Kotani, *Carbon* **2014**, *76*, 266 – 274.
[14] M. Stępień, E. Gońka, M. Żyła, N. Sprutta, *Chem. Rev.* **2017**, *117*, 3479 – 3716.
[15] S. Ito, *J. Synth. Org. Chem. Jpn.* **2019**, *77*, 1128 – 1135.
[16] K. Nakamura, Q.-Q. Li, O. Krejčí, A. S. Foster, K. Sun, S. Kawai, S. Ito, *J. Am. Chem. Soc.* **2020**, *142*, 11363 – 11369.
[17] a) D. Myśliwiec, M. Stępień, *Angew. Chem. Int. Ed.* **2013**, *52*, 1713 – 1717; *Angew. Chem.* **2013**, *125*, 1757 – 1761; b) V. M. Tsefrikas, A. K. Greene, L. T. Scott, *Org. Chem. Front.* **2017**, *4*, 688 – 698; c) P. Kaewmati, Q. Tan, S. Higashibayashi, Y. Yakiyama, H. Sakurai, *Chem. Lett.* **2017**, *46*, 146 – 148; d) S. Higashibayashi, P. Pandit, R. Haruki, S.-i. Adachi, R. Kumai, *Angew. Chem. Int. Ed.* **2016**, *55*, 10830 – 10834; *Angew. Chem.* **2016**, *128*, 10988 – 10992; e) H. Yokoi, Y. Hiraoka, S. Hiroto, D. Sakamaki, S. Seki, H. Shinokubo, *Nat. Commun.* **2015**, *6*, 8215; f) D. Myśliwiec, M. Kondratowicz, T. Lis, P. J. Chmielewski, M. Stępień, *J. Am. Chem. Soc.* **2015**, *137*, 1643 – 1649; g) S. Ito, Y. Tokimaru, K. Nozaki, *Angew. Chem. Int. Ed.* **2015**, *54*, 7256 – 7260; *Angew. Chem.* **2015**, *127*, 7364 – 7368; h) K. Oki, M. Takase, S. Mori, A. Shiotari, Y. Sugimoto, K. Ohara, T. Okujima, H. Uno, *J. Am. Chem. Soc.* **2018**, *140*, 10430 – 10434; i) Y. Tokimaru, S. Ito, K. Nozaki, *Angew. Chem. Int. Ed.* **2018**, *57*, 9818 – 9822; *Angew. Chem.* **2018**, *130*, 9966 – 9970; j) H. Yokoi, S. Hiroto, D. Sakamaki, S. Seki, H. Shinokubo, *Chem. Sci.* **2018**, *9*, 819 – 824; k) X. Tian, L. M. Roch, N. Vanthuyne, J. Xu, K. K. Baldridge, J. S. Siegel, *Org. Lett.* **2019**, *21*, 3510 – 3513; l) N. Deng, G. Zhang, *Org. Lett.* **2019**, *21*, 5248 – 5251; m) Q. Tan, P. Kaewmati, S. Higashibayashi, M. Kawano, Y. Yakiyama, H. Sakurai, *Bull. Chem. Soc. Jpn.* **2018**, *91*, 531 – 537; n) M. Takeda, S. Hiroto, H. Yokoi, S. Lee, D. Kim, H. Shinokubo, *J. Am. Chem. Soc.* **2018**, *140*, 6336 – 6342; o) M. Saito, H. Shinokubo, H. Sakurai, *Mater. Chem. Front.* **2018**, *2*, 635 – 661; p) T. Nagano, K. Nakamura, Y. Tokimaru, S. Ito, D. Miyajima, T. Aida, K. Nozaki, *Chem. Eur. J.* **2018**, *24*, 14075 – 14078; q) Q. Tan, S. Higashibayashi, S. Karanjit, H. Sakurai, *Nat. Commun.* **2012**, *3*, 891; r) L. Zhou, G. Zhang, *Angew. Chem. Int. Ed.* **2020**, *59*, 8963 – 8968; *Angew. Chem.* **2020**, *132*, 9048 – 9053.
[18] a) U. H. F. Bunz, J. Freudenberg, *Acc. Chem. Res.* **2019**, *52*, 1575 – 1587; b) Z. Liang, Q. Tang, R. Mao, D. Liu, J. Xu, Q. Miao, *Adv. Mater.* **2011**, *23*, 5514 – 5518.
[19] H. Sakurai, T. Daiko, T. Hirao, *Science* **2003**, *301*, 1878 – 1878.
[20] V. M. Tsefrikas, S. Arns, P. M. Merner, C. C. Warford, B. L. Merner, L. T. Scott, G. J. Bodwell, *Org. Lett.* **2006**, *8*, 5195 – 5198.
[21] T. Kirschbaum, F. Rominger, M. Mastalerz, *Angew. Chem. Int. Ed.* **2020**, *59*, 270 – 274; *Angew. Chem.* **2020**, *132*, 276 – 280.
[22] G. Zhang, V. Lami, F. Rominger, Y. Vaynzof, M. Mastalerz, *Angew. Chem. Int. Ed.* **2016**, *55*, 3977 – 3981; *Angew. Chem.* **2016**, *128*, 4045 – 4049.
[23] a) L. Di Bari, S. Guillarme, S. Hermitage, D. A. Jay, G. Pescitelli, A. Whiting, *Chirality* **2005**, *17*, 323 – 331; b) L. Di Bari, G. Pescitelli, P. Salvadori, M. Rovini, M. Anzini, A. Cappelli, S. Vomero, *Tetrahedron: Asymmetry* **2006**, *17*, 3430 – 3436.
[24] C. M. Cardona, W. Li, A. E. Kaifer, D. Stockdale, G. C. Bazan, *Adv. Mater.* **2011**, *23*, 2367 – 2371.

Manuscript received: June 11, 2020
Accepted manuscript online: June 15, 2020
Version of record online: October 12, 2020